http://jbcp.shahed.ac.ir 10.22070/jbcp.2020.5077.1127

Open Access Research Article

Journal of Basic and Clinical Pathophysiology
Print ISSN: 2322-1895, **Online ISSN:** 2345-4334
Vol.8, No.1, June 2020

A Semiannual Publication of
Shahed University Press

Selenium nanoparticles inclusion into chitosan hydrogels act as a chemical inducer for differentiation of PC12 cells into neuronal cells

Hamed Amani[1], Hanif Kazerooni[2], Hossein Hassanpoor[3]*

1. Department of Medical Nanotechnology, Faculty of Advanced Technologies in Medicine, Iran University of Medical Science, Tehran, Iran
2. Department of Chemical Engineering, Amirkabir University of Technology (Tehran Polytechnic), Tehran, Iran
3. Department of Cognitive Science, Dade Pardazi, Shenakht Mehvar, Atynegar (DSA) Institute, Tehran, Iran

Abstract

Background and Objective: Biomaterials and nanomaterials have generated a great opportunity in regenerative medicine. Neurological disorders can result in permanent and severe derangement in motor and sensory functions. This study was conducted to examine the effects of selenium nanoparticles (Se NPs) as a chemical inducer for differentiation of PC12 cells into sympathetic-like neurons characterized by neurite outgrowth.

Materials and Methods: Size, surface charge, the shape of Se NPs and the morphology of hydrogels were characterized by dynamic light scattering (DLS), zeta sizer, transmission electron microscopy (TEM) and scanning electron microscopy (SEM), respectively. DAPI staining, RT-PCR and western blot assays were used to evaluate cell attachment and mRNA and protein levels of neuronal markers, respectively.

Results: The hydrodynamic size of Se NPs was about 33.55 nm and their surface charge was shifted from -24 to +3.4 mV. The morphological characterization demonstrated monodisperse spherical particles after coating with BSA. SEM images demonstrated that chitosan hydrogel containing Se NPs has suitable pore sizes for penetration of cells. DAPI staining and live/dead assay demonstrated the ability of cell attachment and biocompatibility of hydrogel, respectively. RT-PCR and western blot assays showed that neurite extension of differentiated PC12 cells can be linked to significantly increased mRNA levels of Map2, β-tubulin, increased protein levels of neurofilament-200 (NF200) as neuronal markers and decreased protein levels of ki67 protein as a proliferation marker.

Conclusion: Collectively, our findings show that Se NPs can act as a chemical inducer for the differentiation of PC12 cells into sympathetic-like neurons in chitosan hydrogels **Key words:** Sodium arsenite, Oxidative damage, Seizure, Pentylenetetrazole

Keywords: Selenium nanoparticles, Neuronal differentiation, Chitosan hydrogels, Nerve regeneration

1. Introduction

Owing to the inadequate intrinsic regenerative ability of the nervous system, especially the central nervous system (CNS), neurological disorders might result in permanent and severe derangement in motor and sensory functions (1-3). Although peripheral nerves might be able to regenerate after injury, it is not efficient in the case of the nerve damage with long distance (4-6). Though the gold standard treatment for peripheral nerve injury is autologous nerve grafting, it has several drawbacks including the possibility of a mismatch between donor and recipient nerves, pain, scar formation, lack and limited availability of donor tissue, and a necessity for additional surgery to provide the donor nerve (7,8). To overcome these limitations, different biomaterials and nanomaterials have been introduced by researchers (9,10). Chitosan is a natural cationic polysaccharide polymer that can be formed by the alkaline N-deacetylation of chitin and is present in the exoskeletons of insects. The unique properties of chitosan such as excellent biocompatibility, facile production, antibacterial, and

Received: 31 Dec 2019**, Accepted:** 27 Mar 2020, **Available online:** 23 June 2020
Corresponding Author: Hossein Hassanpoor **E-mail:** hossein.hassanpoor@gmail.com

antimicrobial activity make it a good candidate for nerve tissue engineering purposes (11, 12). It has been reported that selenium is an essential trace element to human health that can participate in reinforcement of endogenous antioxidant system and regulation of neurogenesis (13, 14).

On the other hand, selenium nanoparticles (Se NPs) have been known as promising tools for fighting against neurological disorders such as Alzheimer's disease by suppressing amyloid-β aggregation (15). Currently, it has been reported that Se NPs can act as osteogenic chemical inducers and improve differentiation of mesenchymal stem cells (MSCs) into osteoblasts (16). Here, we went on to design a chitosan hydrogel containing Se NPs and evaluate its effects on the behavior of PC12 cells and their differentiation into sympathetic-like neurons characterized by neurite outgrowth.

2. Materials and Methods

2.1. Synthesis of Se NPs

Initially, 1800 µL of 0.1 M selenious acid 98% (Sigma-Aldrich) was added to 10 mL of deionized (DI) water containing 25 mg/mL of BSA under continuous stirring. In the next step, 3 mL of aqueous 0.1 M ascorbic acid solution (A92902, Sigma-Aldrich) was added dropwise. Color change from colorless to pale yellow, then yellow, and finally into the orange-red confirmed synthesis of Se NPs.

2.2. Characterizations of nanoparticles

A Nano-ZS instrument (Malvern Zeta sizer Nano ZS90, Worcestershire, UK) was used to determine the size distribution and zeta potential of the Se NPs. Likewise, the morphology and stability of Se NPs were evaluated by transmission electron microscopy (TEM, H-7650) at an accelerating voltage of 80 kV. In order to prepare samples for TEM, a droplet of diluted nanoparticles was dropped onto carbon-coated copper grids and then samples were dried at room temperature for several days.

2.3. Preparation of hydrogels

Initially to obtain a pale yellow viscous chitosan solution, 1.5 g of chitosan was dissolved in 20.0 mL of 2.0% aqueous acetic acid under continuous stirring at room temperature for overnight. In order to provide a uniform dispersion of solution and to hamper aggregation during stirring, several drops of 0.5% tween-80 were added to the resulting solution. In the next step, 1.0 mL of 0.1% aqueous glutaraldehyde solution was added and samples were dried overnight at room temperature to obtain cross-linked chitosan hydrogels. In the case of hydrogels containing particles, 250 µl of Se NPs (250 µg/mL) was added to pale yellow viscous chitosan solution 30 min before the addition of 0.1% aqueous glutaraldehyde solution.

2.4. Characterization of hydrogels containing Se NPs

The morphology of the scaffolds was investigated by scanning electron microscopy (SEM AIS2100, Seron Technology, South Korea). In order to prepare samples, they were sputter coated with gold at an accelerating voltage of 20 kV.

2.5. Cell culture

Cells were counted before each experiment to provide the required cell density. PC12 cells were obtained from Pasteur Institute of Iran and cultured in RPMI 1640 medium containing 10% fetal calf serum (Gibco), 1% penicillin-streptomycin at 37°C in a humidified 5% CO2 atmosphere. An equal amount of cells was loaded on hydrogels after 2-4 passages.

2.6. Cell adhesion

To evaluate the number of attached cells on the surface of hydrogel, nucleus staining by 4′, 6-diamidino-2-phenylindole (DAPI, Sigma) was used. First, 2×104 cells were seed on hydrogels (0.5×0.5 cm2). After 48 h, PC12 cells were stained by DAPI, then washed with PBS and were visualized under fluorescence microscopy (Nikon Eclipse 230 80i).

2.7. Cell viability

Five days after cell culture (2×104 cells/cm2) on the hydrogels, they were washed with PBS and incubated in calcein AM and ethidium homodimer solution according to the manufacturer's instructions. Then, cells were washed with phosphate buffer saline (PBS) for another time and were visualized under fluorescence microscopy (Nikon Eclipse 230 80i). The color of live cells was green whereas the color of dead cells was red.

2.8. Real time PCR

Briefly, total RNAs were extracted using TRIzol (Invitrogen) and then were reverse transcribed to produce single-strand cDNA by a Dart cDNA kit (EURx Company, Poland) according to the manufacturer's protocol. SYBR Premix Ex Taq II (Takara, Japan) was used to detect PCR products. Temperature cycling was 94°C for 30 s, 56°C for 30 s, and 68°C for 1 min and repeated for 45 cycles. Relative changes in gene expression were calculated based on the $2^{-\Delta\Delta CT}$ method. Glyceraldehyde 3-phosphate dehydrogenase (GAPDH) was used as an internal control. Primers used in this study were Map2

(F) CAAAGTTTATGGGGAGAAAAGGGA, Map2 (R) CAAGGGCAATAGAATCAAGGCAAG; β-tubulin (F) CCAGCGGCAACTATGTAGG, β-tubulin (R) CACCACTCTGACCAAAGATAAAG; GAPDH (F) AGTTCAACGGCACAGTCAAG, GAPDH (R) TACTCAGCACCAGCATCACC.

2.9. Western blot assay

Briefly, samples were homogenized in RIPA buffer (protease and phosphatase inhibitor) and after centrifugation at 13,000 g for 20 min, the total protein concentrations were measured by the Nanodrop equipment (NANODROP OneC, Thermo Scientific). After loading the equal amounts of proteins (50 µg) into the electrophoresis chamber in 10-15 % SDS-PAGE, the separated soluble proteins were transferred onto PVDF membrane. In the next step, non-specific sites were blocked utilizing a fresh blocking buffer containing 0.1 % Tween-20, 5 % BSA, and Tris-buffered saline (pH 7.4). Then, the membranes were incubated with the primary antibodies including Anti-Ki-67 Antibody (1:500, Bosterbio, USA) and Anti-NF200 antibody (1:1000, MyBioSource, USA) followed by anti-rabbit IgG peroxidase-conjugated secondary antibody (1:3000, Cell Signaling Technology, Danvers, MA, USA) for 1 h. Chemiluminescent HRP substrate (Millipore) was used as a detector of immunoreactivity and finally, the membranes were exposed to Kodak X-OMAT films for 5 min. Internal control for western blot assay was β-actin (1:1000, β-Actin Antibody #4967, Cell Signaling Technology). The ratio expression of each protein to the expression of the β-actin was determined using Alpha Ease ® FC Imaging System based on their optical densities.

2.10. Statistical analysis

Data were expressed as means ± standard deviation (SD). Analysis of data was performed utilizing GraphPad Prism-5 statistic software (LaJolla, CA, USA). Two-tailed student's t-test was served to analyze the difference between the two groups. Values of $P < 0.05$ were accepted to be significant in all cases.

3. Results

3.1. Characterization of Se NPs

To characterize the size distribution, surface charge and morphology of particles, various spectroscopic and microscopic methods were applied. As shown in Figure 1A, DLS demonstrated that the hydrodynamic size of particles was 33.55 nm. Likewise, zeta sizer showed that surface charge of bare nanoparticle was -24 mV that was shifted to +3.4 after coating with BSA. As depicted in Figure 1B and 1C, TEM images demonstrated that bare Se NPs were aggregated owing to their high surface free energy. Monodisperse spherical particles with high stability were observed after coating with BSA.

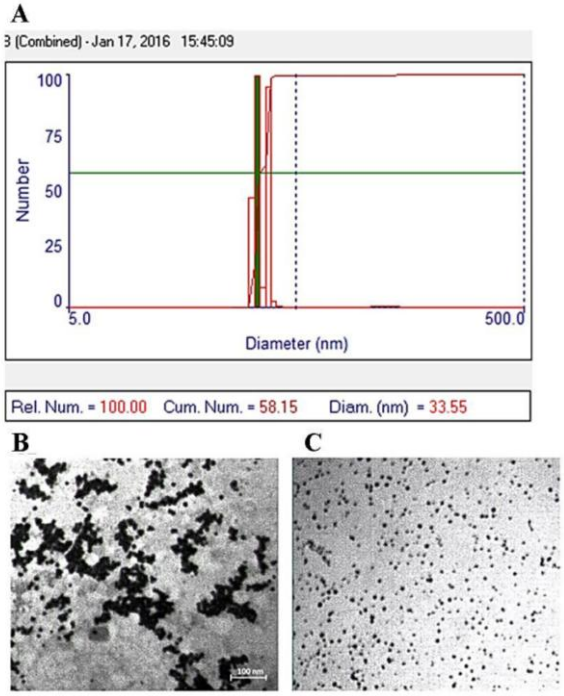

Figure 1. Characterization of Se NPs. A) The hydrodynamic size of Se NPs. TEM images of B) bare and C) BSA coated Se NPs.

3.2. Effects of Se NPs in two-dimensional microenvironment on the behavior of PC12 cells

Five days after treatment with 250 µg/mL dose of Se NPs, PC12 cells were spread out and neurite outgrowth was found that was not significant compared to control (Figures 2A and 2B). Ten days after treatment with 250 µg/mL dose of Se NPs, neuron-like PC12 cells were spread out and significant promotion of neurite outgrowth was found compared to control (Figures 2C and 2D).

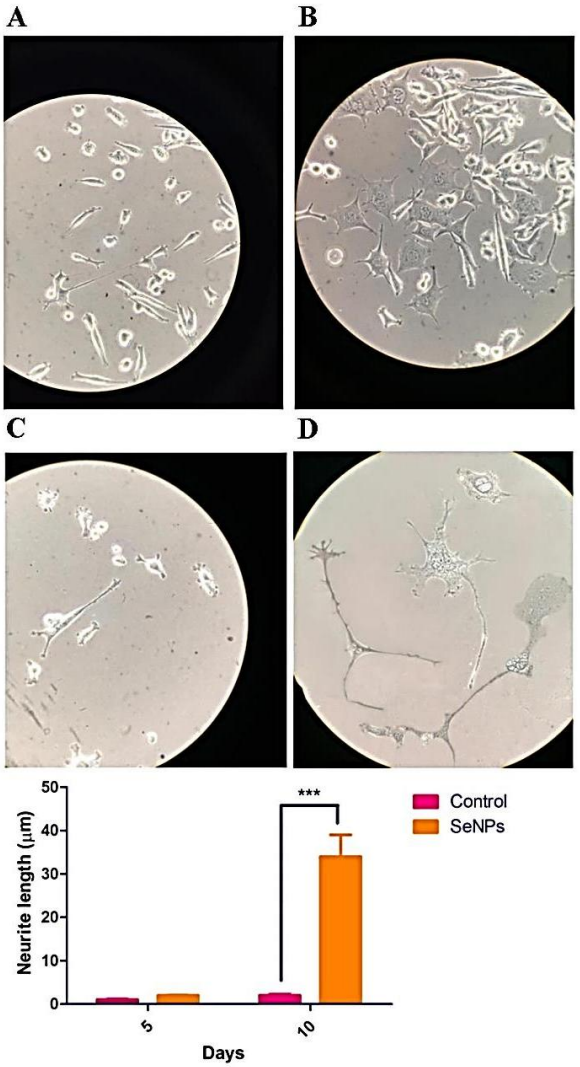

Figure 2. The behavior of PC12 cells after post-treatment with 250 µg/mL dose of Se NPs. A) Control after 5 days, B) 5 days after post-treatment with 250 µg/mL dose of Se NPs. C) Control after 10 days and D) 10 days after post-treatment with 250 µg/mL dose of Se NPs (***P<0.001 vs. control after 10 days).

3.3. Characterization of hydrogels

SEM images showed that hydrogels containing Se NPs have porous structures with interconnected holes, indicating the possibility for penetration, attachment, and growth of cells (Figure 3).

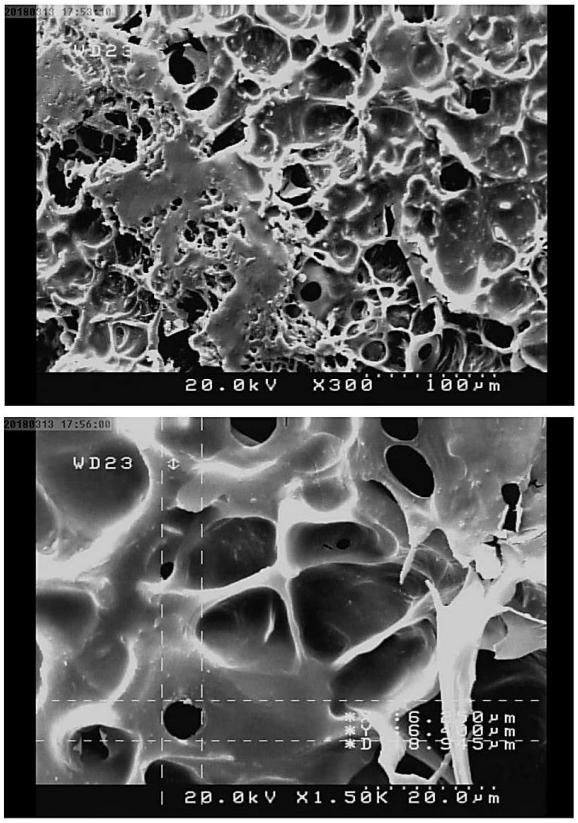

Figure 3. Characterization of hydrogels. SEM images confirmed that chitosan hydrogels containing Se NPs are porous structures with suitable pore sizes for cell penetration, migration, and attachment.

3.4. Cell attachment

DAPI staining showed that PC12 cells could attach to the hydrogels containing Se NPs after 48 h of cell seeding. These results demonstrated that the pore sizes of hydrogel were suitable and cells can penetrate into the structure of hydrogel (Figure 4).

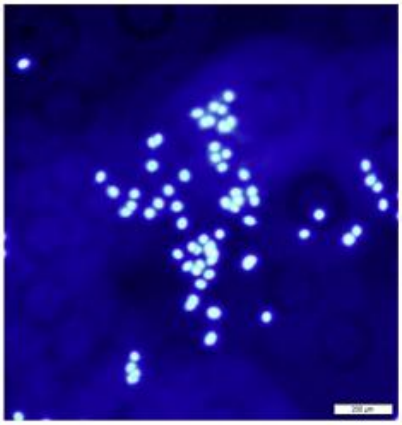

Figure 4. Evaluation of cell adhesion. DAPI staining showed that chitosan hydrogels containing Se NPs are suitable structures for cell attachment (Scale bar: 200 µm).

3.5. Cell viability

A live/ dead assay kit was used to determine the viability of cells within hydrogels. Cells that lost membrane integrity and were not viable stained red whereas the viable cells stained green. As shown in Figures 5A and 5B, dead cells were low in both hydrogels and hydrogels containing Se NPs and no significant differences were found between the two groups (Figure 5).

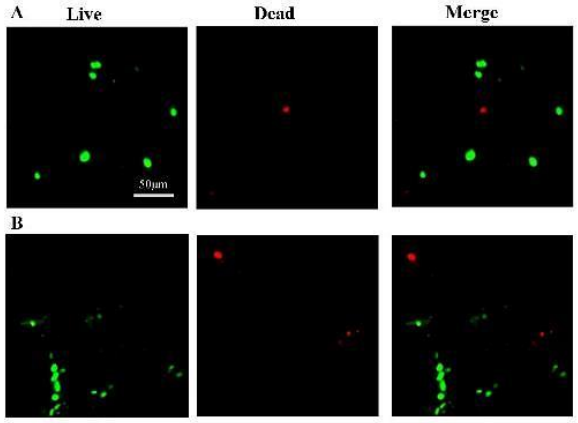

Figure 5. Viability of PC12 cells after 48 h. A) Control, B) chitosan hydrogels containing Se NPs. There were no significant differences between two groups (green: live cells; red: dead cells).

3.6. The expression of neural markers

Fluorescence images of PC12 cells on the chitosan hydrogels containing Se NPs showed that these structures decreased proliferation and enhanced differentiation (Figures 6A and 6B). To confirm that chitosan hydrogels containing Se NPs can contribute to the differentiation of PC12 cells into sympathetic-like neurons, the mRNA levels of neuronal markers such as Map2 and β-tubulin were measured by RT-PCR assay. As depicted in Figures 6C and 6D, the expression of both markers significantly increased in cells seeded into chitosan hydrogels containing Se NPs compared to control. To approve the findings of RT-PCR assay, we also performed western blot assay to evaluate protein expressions of NF200 as a neuronal differentiation marker and ki67 as a proliferation marker. Western blot analysis showed that the expression of NF200 was significantly increased in cells seeded into hydrogels containing Se NPs compared to control, while ki67 protein demonstrated a significantly lower expression in cells seeded into chitosan hydrogels containing Se NPs as compared to control (Figure 6E).

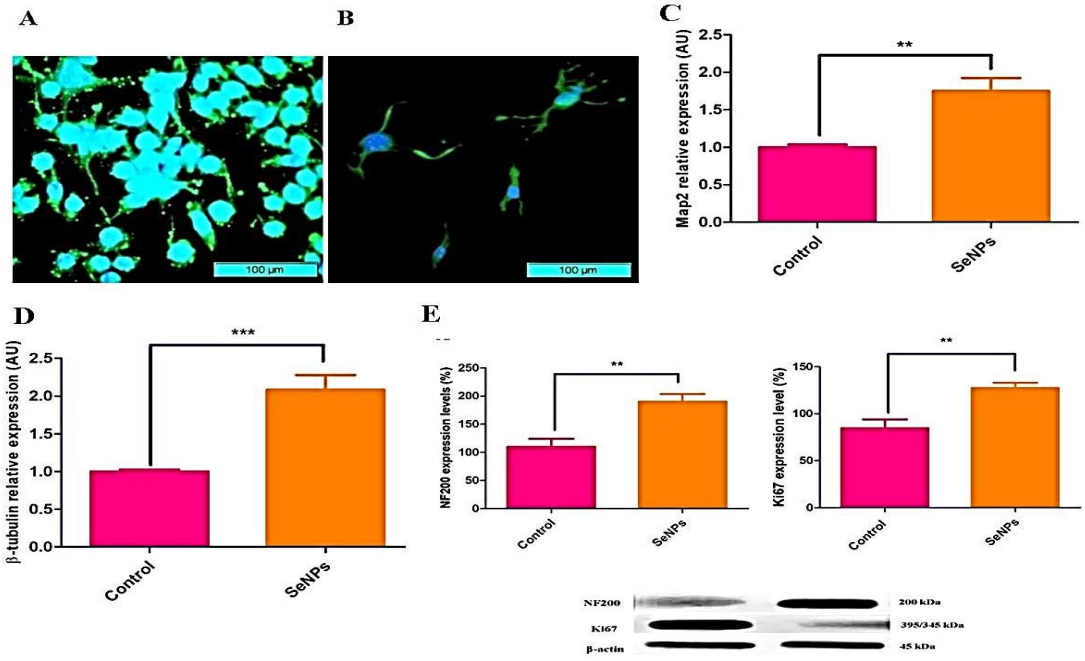

Figure 6. The effects of Se NPs on the proliferation and differentiation markers into the structure of chitosan hydrogels. Fluorescence images of A) control and B) chitosan hydrogels containing Se NPs. The mRNA levels of neuronal markers including C) Map2 (** P<0.01 vs. control) and D) β-tubulin (*** P<0.001 vs. control). E) The protein levels of neuronal differentiation markers (NF200) and proliferation markers (ki67 protein) (** P<0.01 vs. control). NPs.

4. Discussion

Unlike many other scaffolds that need expensive and laborious fabrication techniques, we designed a hydrogel containing Se NPs from chitosan, an inexpensive polymer, for nervous tissue engineering purposes. Here, we fabricated chitosan hydrogels without and with Se NPs to examine the effects of these nanoparticles on behaviors of PC12 cells such as viability, proliferation, and differentiation in the absence of nerve growth factor (NGF). Chitosan was chosen to prepare hydrogels because it is a biocompatible polymer with anti-bacterial effects that can be used as a nanocarrier for nerve growth factors (17-20). Many previous studies have shown that Se NPs affect cell behavior under different pathological conditions owing to their antioxidant properties (21, 22). It has been reported that Se NPs possess a 7-fold lower acute toxicity than sodium selenite in mice and their biocompatibility is more than other compounds of selenium. Likewise, Se NPs with a diameter of less than 100 nm possess more antioxidant properties and have extensively used as food additives, antimicrobial and anticancer agents (23-25). In keeping with these previous studies, our findings showed that the size of Se NPs was 33.55 nm which indicates they possess suitable antioxidant and physicochemical properties. A previous study has shown that positive surface charge of Se NPs improved cellular uptake and their efficiency for the treatment of cancer cells in vitro (26). In agreement with this study, our findings showed that the coating of Se NPs with BSA increased their stability and shifted their surface charge from negative to positive. It is well documented that Se NPs can act as chemical inducer and can improve the differentiation of MSCs into osteoblasts. Moreover, it has been recognized that Se NPs can cross the blood-brain barrier (BBB) and exert positive effects on the nerve system by suppressing the generation of reactive oxygen species (ROS) (27).

To examine if Se NPs can affect the behavior of PC12 cells, we added it to cell culture flask and found it strongly stimulated neurite growth and inhibited cell proliferation after 10 days. In order to obtain greater insights on the function of Se NPs as a neuronal chemical inducer, we examined expression of mRNA and proteins of some proteins. Our finding demonstrated that neurite extension of differentiated PC12 cells was associated with increased expression levels of neurofilament 200 (NF200), β-tubulin and Map2. Our finding was in agreement with a work by tian et al that reported that increased expression of NF200 by PC12 cells proved differentiation of them into sympathetic-like neurons characterized by neurite outgrowth (28). According to our study, Chen et al reported that the differentiation of PC12 into neuronal cells onto a three-dimensional electrical conductive scaffold from biomaterial-based carbon microfiber sponge is associated with expression of Map2 (29). On the other hand, we found that Se NPs inhibited the proliferation of PC12 cells. To confirm the inhibitory effect of Se NPs on the proliferation of PC12 cells, ki67 protein was measured as a marker of proliferation (30). In keeping with our findings, many previous studies have shown that Se NPs possess inhibitory effects on the proliferation of tumor cells and PC12 cells were cloned from a pheochromocytoma tumor (31-33).

In conclusion, our findings showed that Se NPs can act as a potent chemical inducer for differentiation of PC12 cells into sympathetic-like neurons characterized by neurite outgrowth. Here, we found that chitosan hydrogels containing Se NPs could act as biocompatible three-dimensional structures for the regeneration of damaged nerves.

Acknowledgements

No specific funding has been provided for the research.

Conflict of Interest:

The authors declare that they have no conflicts of interest.

References

1. Ong W, Pinese C, Chew SY. Scaffold-mediated sequential drug/gene delivery to promote nerve regeneration and remyelination following traumatic nerve injuries. Advanced Drug Delivery Reviews 2019.
2. Poplawski G, Ishikawa T, Brifault C, Lee-Kubli C, Regestam R, Henry KW, et al. Schwann cells regulate sensory neuron gene expression before and after peripheral nerve injury. Glia 2018;66(8):1577-90.
3. Anderson MA, Burda JE, Ren Y, Ao Y, O'Shea TM, Kawaguchi R, et al. Astrocyte scar formation aids central nervous system axon regeneration. Nature 2016;532(7598):195.
4. Bonfanti L. From hydra regeneration to human brain structural plasticity: a long trip through narrowing roads. The Scientific World Journal 2011;11:1270-99.
5. Schuh CM, Day AG, Redl H, Phillips J. An optimized collagen-fibrin blend engineered neural tissue promotes peripheral nerve repair. Tissue Engineering Part A 2018;24(17-18):1332-40.
6. Meyer C, Stenberg L, Gonzalez-Perez F, Wrobel S, Ronchi G, Udina E, et al. Chitosan-film

enhanced chitosan nerve guides for long-distance regeneration of peripheral nerves. Biomaterials 2016;76:33-51.

7. Santos D, Wieringa P, Moroni L, Navarro X, Valle JD. PEOT/PBT guides enhance nerve regeneration in long gap defects. Advanced Healthcare Materials 2017;6(3):1600298.
8. Gu X, Ding F, Yang Y, Liu J. Construction of tissue engineered nerve grafts and their application in peripheral nerve regeneration. Progress in Neurobiology 2011;93(2):204-30.
9. Vishnoi T, Singh A, Teotia AK, Kumar A. Chitosan-gelatin-polypyrrole cryogel matrix for stem cell differentiation into neural lineage and sciatic nerve regeneration in peripheral nerve injury model. ACS Biomaterials Science & Engineering 2019.
10. Dalamagkas K, Tsintou M, Seifalian A. Advances in peripheral nervous system regenerative therapeutic strategies: a biomaterials approach. Materials Science and Engineering: C 2016; 65:425-32.
11. Bąk M, Gutkowska ON, Wagner E, Gosk J. The role of chitin and chitosan in peripheral nerve reconstruction. Polymers in Medicine 2017; 47(1):43-7.
12. Zhao Y, Wang Y, Gong J, Yang L, Niu C, Ni X, et al. Chitosan degradation products facilitate peripheral nerve regeneration by improving macrophage-constructed microenvironments. Biomaterials 2017;134:64-77.
13. Cardoso BR, Roberts BR, Bush AI, Hare DJ. Selenium, selenoproteins and neurodegenerative diseases. Metallomics 2015;7(8):1213-28.
14. Flohé L. Selenium and human health: snapshots from the frontiers of selenium biomedicine. Selenium and tellurium chemistry: Springer; 2011: 285-302.
15. Zhang J, Zhou X, Yu Q, Yang L, Sun D, Zhou Y, et al. Epigallocatechin-3-gallate (EGCG)-stabilized selenium nanoparticles coated with Tet-1 peptide to reduce amyloid-β aggregation and cytotoxicity. ACS Applied Materials & Interfaces 2014;6(11):8475-87.
16. Zheng C, Wang J, Liu Y, Yu Q, Liu Y, Deng N, et al. Functional selenium nanoparticles enhanced stem cell osteoblastic differentiation through BMP signaling pathways. Advanced Functional Materials 2014;24(43):6872-83.
17. Mili B, Das K, Kumar A, Saxena A, Singh P, Ghosh S, et al. Preparation of NGF encapsulated chitosan nanoparticles and its evaluation on neuronal differentiation potentiality of canine mesenchymal stem cells. Journal of Materials Science: Materials in Medicine 2018;29(1):4.
18. Baniasadi H, SA AR, Mashayekhan S. Fabrication and characterization of conductive chitosan/gelatin-based scaffolds for nerve tissue engineering. International Journal of Biological Macromolecules 2015;74:360-6.
19. Subhi H, Hakimi I, Jie NTL, Reza F, Husein A, Nurul AA. Effect of chitosan on antibacterial activity of gypsum-based biomaterial compared to two dental liners. Journal of International Oral Health 2019;11(3):118.
20. Vaz JM, Pezzoli D, Chevallier P, Campelo CS, Candiani G, Mantovani D. Antibacterial coatings based on chitosan for pharmaceutical and biomedical applications. Current Pharmaceutical Design 2018;24(8):866-85.
21. Liu W, Li X, Wong Y-S, Zheng W, Zhang Y, Cao W, et al. Selenium nanoparticles as a carrier of 5-fluorouracil to achieve anticancer synergism. ACS Nano 2012;6(8):6578-91.
22. Sakr TM, Korany M, Katti KV. Selenium nanomaterials in biomedicine—An overview of new opportunities in nanomedicine of selenium. Journal of Drug Delivery Science and Technology 2018;46:223-33.
23. Kong H, Yang J, Zhang Y, Fang Y, Nishinari K, Phillips GO. Synthesis and antioxidant properties of gum arabic-stabilized selenium nanoparticles. International Journal of Biological Macromolecules 2014;65:155-62.
24. Cremonini E, Zonaro E, Donini M, Lampis S, Boaretti M, Dusi S, et al. Biogenic selenium nanoparticles: characterization, antimicrobial activity and effects on human dendritic cells and fibroblasts. Microbial Biotechnology 2016;9(6):758-71.
25. Menon S, KS SD, Santhiya R, Rajeshkumar S, Kumar V. Selenium nanoparticles: A potent chemotherapeutic agent and an elucidation of its mechanism. Colloids and Surfaces B: Biointerfaces 2018;170:280-92.
26. Yu B, Zhang Y, Zheng W, Fan C, Chen T. Positive surface charge enhances selective cellular uptake and anticancer efficacy of selenium nanoparticles. Inorganic Chemistry 2012;51(16):8956-63.
27. Yang L, Sun J, Xie W, Liu Y, Liu J. Dual-functional selenium nanoparticles bind to and inhibit amyloid β fiber formation in Alzheimer's disease. Journal of Materials Chemistry B 2017;5(30):5954-67.

28. Tian L, Prabhakaran MP, Hu J, Chen M, Besenbacher F, Ramakrishna S. Synergistic effect of topography, surface chemistry and conductivity of the electrospun nanofibrous scaffold on cellular response of PC12 cells. Colloids and Surfaces B: Biointerfaces 2016;145:420-9.

29. Chen X, Wu Y, Ranjan VD, Zhang Y. Three-dimensional electrical conductive scaffold from biomaterial-based carbon microfiber sponge with bioinspired coating for cell proliferation and differentiation. Carbon 2018;134:174-82.

30. Li N, Zhang Q, Gao S, Song Q, Huang R, Wang L, et al. Three-dimensional graphene foam as a biocompatible and conductive scaffold for neural stem cells. Scientific Reports 2013;3:1604.

31. Greene LA, Tischler AS. Establishment of a noradrenergic clonal line of rat adrenal pheochromocytoma cells which respond to nerve growth factor. Proceedings of the National Academy of Sciences 1976;73(7):2424-8.

32. Hu Y, Liu T, Li J, Mai F, Li J, Chen Y, et al. Selenium nanoparticles as new strategy to potentiate γδ T cell anti-tumor cytotoxicity through upregulation of tubulin-α acetylation. Biomaterials 2019;222:119397.

33. Ahmed NH, El-Batal AI, Barakat LA, Khirallah SM. Possibility of Selenium Nanoparticles Manufactured by Glycyrrhiza glabra Extract and γ-irradiation to Suppress the Growth of Murine Tumor. Journal of Advance Research in Pharmacy & Biological Science 2019;5(2):01-23.